Superconducting Proximity Effect Probed on a Mesoscopic Length Scale

S. Guéron, H. Pothier, Norman O. Birge,* D. Esteve, and M. H. Devoret
Service de Physique de l'Etat Condensé, Commissariat à l'Energie Atomique, Saclay, F-91191 Gif-sur-Yvette Cedex, France
(Received 12 April 1996)

We have measured by tunneling spectroscopy the electronic density of states in a nonsuperconducting wire in good contact with a superconductor, at distances of 200, 300, and 800 nm from the interface. Closest to the interface, the density of states near the Fermi energy is reduced to 55% of its normal value. At the farthest measurement point, this dip has nearly completely disappeared. We compare our data to predictions based on the Usadel equations. [S0031-9007(96)01337-3]

PACS numbers: 74.50.+r, 73.40.Gk, 73.50.Bk

How does superconducting order propagate spatially? This question motivates the renewed interest in contacts between a nonsuperconducting metal and a superconductor (NS interface) [1]. In the 1960s, the propagation of superconductivity through an NS interface, a phenomenon called the proximity effect, was analyzed within the framework of the Ginzburg-Landau (GL) theory based on a superconducting order parameter $\Psi(x)$ which is a function of space only [2]. While the GL theory predicts well macroscopic equilibrium properties near the transition temperature, it makes no prediction at $T = 0$. Moreover, it does not address the energy dependence of pair correlations and therefore offers no understanding of transport properties. In the case of an NS interface with an applied voltage, such an understanding is provided by an extension of the BCS theory [3] but only in the special case of ballistic electrons. The recent observation of a large modulation in the conductance of a normal diffusive wire in contact with two superconductors with different phases appealed for a more thorough understanding [4]. It is now believed that all the experiments on NS structures can be understood from a unified point of view [5–7] based on the theory of "nonequilibrium superconductivity" [8]. In this general theory, correlations between electrons of opposite spin induced in the normal metal at equilibrium are described by a complex function of both space and energy $\theta(x, E)$. The nonequilibrium superconductivity theory establishes a bridge between the GL theory and the BCS theory. The function $\theta(x, E)$ contains the spatial and energy dependence of the density of states: $n(x, E) = N(0)\mathrm{Re}[\cos\theta(\mathrm{x}, \mathrm{E})]$, where $N(0)$ is the density of states at the Fermi energy for the metal in the normal state. It also gives the GL order parameter via an integral over energy [9]. In this Letter, we report a basic test of the theory: We have measured the density of states $n(x, E)$ as a function of energy in a long normal wire in contact with a superconductor at one end, at different distances from the NS interface, and well below the transition temperature [10].

Tunneling has been used extensively to measure the density of states (DOS) [11]: At zero temperature, the differential conductance $dI/dV(V)$ of a tunnel junction between a normal metal electrode and a metal with a DOS $n(E)$ is, disregarding single-electron charging effects [12], proportional to $n(eV)$. In particular, tunneling spectroscopy has already been applied to the proximity effect, but only in normal metal/superconductor bilayers [13]. In such a confined geometry, the spatial dependence of pair correlations can be neglected and the results were explained without the full arsenal of nonequilibrium superconductivity [14]. In our experiment, on the contrary, the lengths of superconductor and normal metal on either side of the interface are large enough that unperturbed superconducting and normal states are recovered far from the interface, thus forcing a gradient of pair correlations. Figure 1 shows a photograph of our sample, which consists of two similar circuits. On the bottom one, two copper

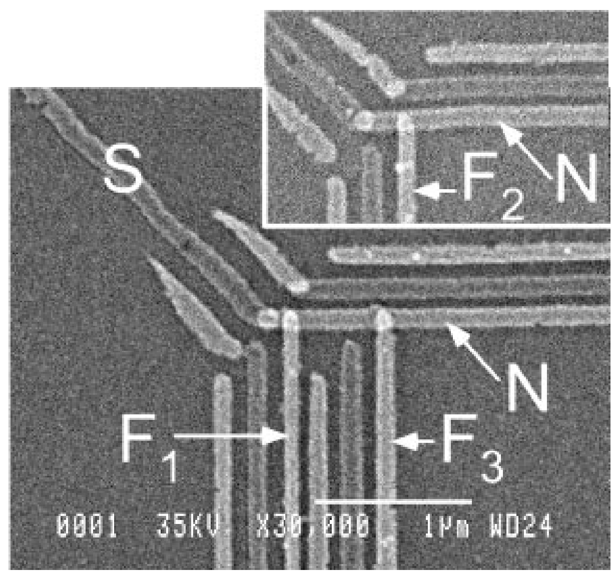

FIG. 1. SEM photograph of the sample: a normal (copper) wire N, horizontal, is in good contact with a superconducting (aluminum) wire S, diagonal on the left, at their overlap. Two normal (copper) fingers, vertical, labeled F_1 and F_3, are connected to the wire through very opaque tunnel barriers. The density of states in the normal wire is given by the differential conductance of the tunnel junction as a function of voltage. On a similar device, a third finger, labeled F_2, is placed at an intermediate distance.

electrodes (called "fingers" in the following, and labeled F_1 and F_3), are in contact through very opaque tunnel barriers (resistances in the MΩ range) with a normal wire *N*, whose left end makes an overlapping contact with a superconductor *S*. On the top circuit, a single finger, labeled F_2, is placed at an intermediate distance from the NS contact, between F_1 and F_3. The three fingers, positioned 200, 300, and 800 nm from the left end of the normal wire, constitute the tunneling spectroscopy probes. Since the quality of the NS contact is known to be a critical parameter in the proximity effect [2], all the layers were deposited through a suspended mask in a single vacuum process [15]. The mask, made of germanium, was fabricated by *e*-beam lithography with reactive ion etching. We first evaporated 20 nm of aluminum perpendicularly to the mask in order to obtain the *S* superconducting electrode. We then immediately evaporated 25 nm of copper at an angle to obtain the *N* normal wire. The angle was chosen so as to produce an overlap with the aluminum electrode on the left, presumably making a good contact. The insulating barrier was grown from two 1.4 nm thick layers of aluminum oxidized in a 80 mbar O_2 (10%) Ar (90%) mixture for 10 min. Lastly, we evaporated 30 nm of copper at an angle to produce the fingers $F_{1,2,3}$. In order to separate the three shadows of the mask, the MAA resist layer carrying the germanium mask was overetched. This was obtained with a low-dose preexposure of the sample around the normal wires and the fingers. The parasitic replicas on both sides of the superconducting electrode produced by the angle evaporations were lifted off in the nonoveretched regions. Two reference structures were simultaneously fabricated on the chip: a long narrow Cu/Al sandwich during the first two evaporation steps (i.e., without oxidation) and an NS tunnel junction formed by the first and third layers (with a thick oxide barrier). The critical temperature of the sandwich is directly related to the transparency of the NS contact [16]; the tunnel junction was used to measure the unperturbed DOS in the *S* film.

The sample was mounted in a copper box thermally anchored to the mixing chamber of a dilution refrigerator. Measurements were performed through properly filtered coaxial lines [17]. Using lock-in detection, we measured the differential conductance dI/dV of each of the three probe junctions as a function of the voltage V applied between the finger and the right end of the normal wire. The differential conductance displayed a *V*-shaped groove at low voltages, which became less pronounced at larger distances from the interface. This behavior is shown in Fig. 2, where we plot the $dI/dV(V)$ characteristic of the F_1, F_2, and F_3 junctions, taken at 20 mK. We have normalized each trace by the conductance $G_i = R_i^{-1} = dI/dV$ measured at $V = 0.3$ meV.

The differential conductance of the reference NS tunnel junction (inset of Fig. 2) is well fitted by a BCS density

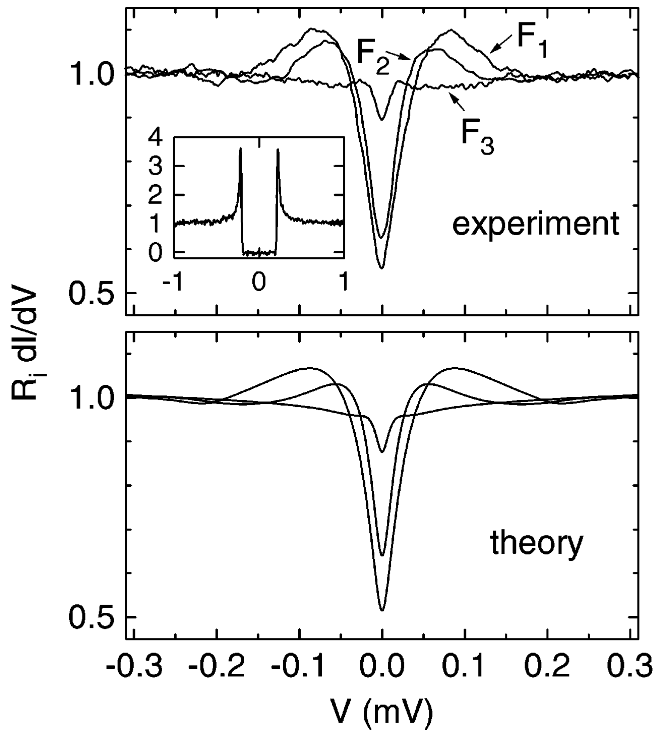

FIG. 2. Top panel: differential conductance of the tunnel junctions at F_1, F_2, and F_3 as a function of the applied voltage V, taken at 20 mK. The ac voltage modulation was kept below 2 μV. The data were normalized by the differential conductance of each junction at $V = 0.3$ mV : $G_1 = 0.19$ μS, $G_2 = 0.38$ μS, $G_3 = 0.27$ μS. Inset, differential conductance of the reference NS tunnel junction. Bottom panel: predicted differential conductance at the three distances to the NS contact obtained from the convolution of the density of states calculated from the Usadel equation [Eq. (1)] with the function $P(E)$ which describes the Coulomb blockade at the junctions. We used $\Delta = 0.212$ meV for the gap of aluminum, $D = 70 \times 10^{-4}$ m^2/s for the diffusion constant of copper, and $\gamma_{sf} = 1.5 \times 10^{10}$ s^{-1} for the spin-flip scattering rate.

of states for the superconducting electrode [18] and yields the energy gap $\Delta = 0.212$ meV.

We repeated the differential conductance measurement of the three fingers with an external magnetic field perpendicular to the chip. In Fig. 3 we present the F_1 data taken at $T = 30$ mK for $H = 0$, 0.06, and 0.1 T. As the field is increased, the groove structure progressively disappears, as shown in the inset of Fig. 3. Above 0.1 T, only a weak, broad-winged, field-independent structure remains (curve *c*). This structure, which extends to 3 mV, is the same for the three fingers. We attribute it, as explained below, to single-electron charging effects. When the temperature was increased (data not shown), the *V*-shaped low-voltage groove structure was progressively washed out, whereas the weak broad-winged structure was unaffected.

We now present the theoretical predictions tested by the experiment. In the theory of nonequilibrium superconductivity, the complex angle $\theta(x, E)$ describing pair

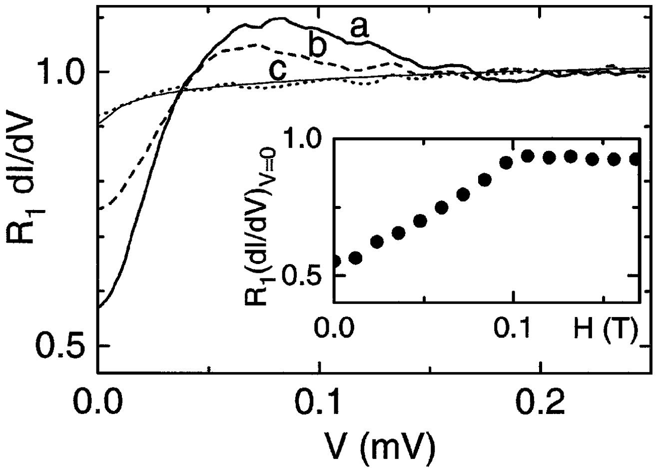

FIG. 3. Differential conductance as a function of the voltage V measured at 30 mK and in a magnetic field $H = 0$ (curve a), 0.06 T (curve b), and 0.1 T (curve c). The thin solid line is a fit of curve c using Eq. (4), in which the DOS $n(x, E)$ was taken constant. It accounts for the influence of single-electron charging effects on the conductance of a tunnel junction between normal electrodes. Inset: zero-voltage conductance of F_1 as a function of the field.

correlations, supplemented with the superconducting phase φ, parametrizes the retarded 2×2 matrix Green function $G^R = (\tau_x \cos\varphi + \tau_y \sin\varphi)\sin\theta + \tau_z \cos\theta$, where $\tau_{x,y,z}$ are the Pauli matrices. At zero energy, θ is real and the superconducting order can be represented as a point on the unit sphere with polar coordinates θ and φ [6]. In this representation, the normal state is at the north pole ($\theta = 0$), and the BCS superconducting state is on the equator ($\theta = \pi/2$) at longitude φ. At finite energy, $\theta = 0$ in the normal state, whereas $\tan\theta_{\rm BCS} = i\Delta/E$. At zero magnetic field, and in an experiment such as ours where the normal metal is in contact with a single superconductor, φ is constant and $\theta(x, E)$ obeys the Usadel equation [8]:

$$\frac{\hbar D}{2}\frac{\partial^2\theta}{\partial x^2} + (iE - \hbar\gamma_{\rm sf}\cos\theta)\sin\theta + \Delta(x)\cos\theta = 0\,. \qquad (1)$$

In this equation $\gamma_{\rm sf}$ is the spin-flip scattering rate and the inelastic scattering rate is assumed to be zero. We will make the approximation that $\gamma_{\rm sf} = 0$ in the superconductor. In a normal metal with no electron-electron interaction, $\Delta = 0$, whereas in a superconductor the pair potential $\Delta(x)$ obeys the self-consistency equation involving the DOS $N_S(0)$ of the superconductor in its normal state, the pairing interaction strength $\mathcal{V}$, and the Debye energy $\hbar\omega_D$:

$$\Delta(x) = N_S(0)\mathcal{V}\int_0^{\hbar\omega_D}\tanh\left(\frac{E}{2k_BT}\right)\mathrm{Im}[\sin\theta]\,dE\,. \qquad (2)$$

Equation (1) is supplemented with boundary conditions: far from the interface, $\theta_N = 0$ in the normal metal, and $\theta_S = \theta_{\rm BCS}$ in the superconductor. At the interface,

$$\sigma_{N,S}\left(\frac{\partial\theta_{N,S}}{\partial x}\right)_{x=0} = \frac{G_{\rm int}}{A}\sin[\theta_S(0,E) - \theta_N(0,E)]\,, \qquad (3)$$

where $\sigma_X = N_X(0)e^2D_X$ is the conductivity and $N_X(0)$ is the DOS at the Fermi energy in electrode X and A is the area of the contact [19]. Although the conductance of the interface $G_{\rm int}$ is not measured, the absence of superconductivity in the sandwich down to 18 mK provides a lower limit: $G_{\rm int} > 2$ S [16]. With such a high conductance, a good approximation is $\theta_S(0,E) = \theta_N(0,E)$. The resolution of the Usadel equation is greatly simplified if Δ is assumed to be independent of x in the superconductor: Eq. (1) then admits a first integral. The DOS is obtained by a second integration performed numerically. We used the value of Δ given by the measurement of the reference NS tunnel junction and the diffusion constant $D_N = 70 \times 10^{-4}$ m^2/s in copper deduced from the conductivity of the wire between F_1 and F_3. The rate $\gamma_{\rm sf}$ was taken as an adjustable parameter. The 1D theory [Eqs. (1) and (3)] does not account for the overlap region of the N and S wires. Nevertheless, the theory produces good agreement with the data if we take the effective NS interface ($x = 0$) to be 20 nm away from the extremity of the normal wire, in the overlap region. We calculate the DOS at the position of the center of each finger. (Calculating the spatially averaged DOS over the width of the finger hardly changes the result.)

For quantitative comparison of the Usadel theory with the experimental data, we must take into account the influence of single-electron charging effects on the conductance. At zero temperature, the differential conductance of the probe tunnel junction at a finger is related to the DOS through

$$\frac{dI}{dV} = \frac{1}{R_t}\int_0^{eV} n(x,E)P(eV - E)\,dE\,, \qquad (4)$$

where R_t is the tunnel resistance of the junction and $P(E)$ is the probability for the electromagnetic environment of the tunnel junction to absorb an energy E [12]. Finite but low temperatures can be accounted for by convolving expression (4) with the derivative of the Fermi function. For a tunnel junction of capacitance C in series with a resistance R such that $\alpha = 2R/(h/e^2) \ll 1$, $P(E) = \alpha/E_0(E/E_0)^{\alpha-1}$ for E smaller than $E_0 = e^2/\pi\alpha C$. The high field data for F_1, F_2, and F_3 are well fitted by Eq. (4) with $n(x,E)$ constant (see fit of curve c in Fig. 3) and yield $\alpha = 0.022$. The fit corresponds to $R = 300\ \Omega$ and $C = 1$ fF, in good agreement with the estimated values.

The comparison between the zero field data taken at 20 mK for the three fingers F_1, F_2, and F_3, and the prediction of Eq. (4) calculated with the DOS $n(x,E)$ previously discussed, is shown in the bottom panel of Fig. 2. The calculation is performed with the value $\gamma_{\rm sf} = 1.5 \times 10^{10}$ s^{-1}, which provides the best overall agreement and is consistent with values found in previous experiments on copper films [20]. As seen in the figure, the theoretical curves reproduce the general features of the experimental data, especially the evolution of the characteristic energy scale with distance from the NS interface [21]. The present theory does not produce maxima as pronounced as those observed, but the exact resolution of the Usadel equation (1) including the gap self-consistency equation (2) improves the agreement [22].

In conclusion, we find that the space and energy dependence of the DOS in a diffusive normal wire in contact with a superconductor is well accounted for by the Usadel equation of the theory of nonequilibrium superconductivity. This DOS is somewhat similar to that of a gapless superconductor. Moreover, it is well known that a supercurrent can flow through a short normal metal wire connected to two superconducting electrodes [23–25]. However, one should not conclude that the proximity effect induces superconductivity in the usual sense: A normal metal wire connected to a single superconductor remains resistive [4,24]. Recent transport calculations [7,26] also based on the Usadel equation account for this seemingly paradoxical behavior.

We acknowledge Yu. Nazarov for introducing us to the theoretical formalism and W. Belzig and C. Bruder for fruitful discussions and communication of their results prior to publication. N. O. B. would like to thank the CEA for its hospitality during the course of this work.

---

*On leave from Michigan State University, East Lansing, MI 48824.

[1] See, for instance, *Proc. of the NATO Adv. Res. Workshop on Mesoscopic Superconductivity* [Physica (Amsterdam) **203B**, 201 (1993)].
[2] G. Deutscher and P. G. de Gennes, in *Superconductivity*, edited by R. D. Parks (Marcel Dekker, New York, 1969), p. 1005.
[3] G. E. Blonder, M. Tinkham, and T. M. Klapwijk, Phys. Rev. B **25**, 4515 (1982).
[4] V. T. Petrashov, V. N. Antonov, P. Delsing, and T. Cleason, Phys. Rev. Lett. **74**, 5268 (1995); P. G. N. de Vegvar, T. A. Fulton, W. H. Mallison, and R. E. Miller, Phys. Rev. Lett. **73**, 1416 (1994).
[5] A. F. Volkov, A. V. Zaitsev, and T. M. Klapwijk, Physica (Amsterdam) **210C**, 21 (1993).
[6] Yu. V. Nazarov, Phys. Rev. Lett. **73**, 1420 (1994).
[7] Yu. V. Nazarov and T. H. Stoof, Phys. Rev. Lett. **76**, 823 (1996); T. H. Stoof and Yu. V. Nazarov, Phys. Rev. B **53**, 14 496 (1996).
[8] A. Schmid, in *Nonequilibrium Superconductivity, Phonons, and Kapitza Boundaries*, edited by K. E. Gray (Plenum Press, New York, 1981), p. 423; J. Rammer and H. Smith, Rev. Mod. Phys. **58**, 323 (1986); A. I. Larkin and Yu. N. Ovchinikov, in *Nonequilibrium Superconductivity*, edited by D. N. Langenberg and A. I. Larkin (North-Holland, Amsterdam, 1986), p. 493; K. D. Usadel, Phys. Rev. Lett. **25**, 507 (1970).
[9] Identification of the expressions for the supercurrent in the GL theory and the nonequilibrium superconductivity theory yields $(\hbar e^*/m^*)[\Psi(x)]^2 = (e/2)N(0)D\int_{-\infty}^{+\infty} dE[1 - 2f(E)]\mathrm{Im}[\sin^2\theta(\mathrm{x},\mathrm{E})]$, where D is the diffusion constant and $f(E)$ the Fermi function.
[10] A complementary experiment was performed by S. H. Tessmer, D. J. Van Harlingen, and J. W. Lyding, Phys. Rev. Lett. **70**, 3135 (1993), on the DOS in thin ballistic N islands on an S substrate.
[11] J. M. Rowell, in *Tunneling Phenomena in Solids*, edited by E. Burstein and S. Lundqvist (Plenum, New York, 1969), p. 385; T. Claeson, *ibid.*, p. 443.
[12] M. H. Devoret, D. Esteve, H. Grabert, G.-L. Ingold, H. Pothier, and C. Urbina, Phys. Rev. Lett. **64**, 1824 (1990); G.-L. Ingold and Yu. V. Nazarov, in *Single Charge Tunneling*, edited by H. Grabert and M. H. Devoret (Plenum Press, New York, 1992), p. 21.
[13] C. J. Adkins and B. W. Kington, Phys. Rev. **177**, 777 (1969); J. R. Toplicar and D. K. Finnemore, Phys. Rev. B **16**, 2072 (1977); A. Kastalsky, L. H. Greene, J. B. Barner, and R. Bhat, Phys. Rev. Lett. **64**, 958 (1990).
[14] W. L. McMillan, Phys. Rev. **175**, 537 (1968).
[15] G. J. Dolan and J. H. Dunsmuir, Physica (Amsterdam) **152A**, 7 (1988).
[16] A. A. Golubov, in *Superconducting Superlattices and Multilayers*, edited by I. Bozovic, SPIE Proceedings Vol. 215 (SPIE, Bellingham, WA, 1994), p. 353.
[17] D. Vion, P. F. Orfila, P. Joyez, D. Esteve, and M. H. Devoret, J. Appl. Phys. **77**, 2519 (1995).
[18] M. Tinkham, *Introduction to Superconductivity* (McGraw Hill, New York, 1985), p. 41.
[19] S. Yip, Phys. Rev. B **52**, 15 504 (1995).
[20] B. Pannetier, J. Chaussy, and R. Rammal, Phys. Scr. **T13**, 245 (1986).
[21] At distances x from the NS interface of the order of $\sqrt{\hbar D/\Delta} \approx 140$ nm, the dominant energy scale of the spectrum is the gap Δ; at larger distances, the characteristic energy is $\hbar D/x^2$ and the spectrum is rounded by the spin-flip scattering rate γ_{sf}.
[22] W. Belzig, C. Bruder, and G. Schön, Phys. Rev. B (to be published).
[23] A. L. De Lozanne and M. R. Beasley, in *Nonequilibrium Superconductivity*, edited by D. N. Langenberg and A. I. Larkin (North-Holland, Amsterdam, 1986), p. 111.
[24] H. Courtois, Ph. Gandit, and B. Pannetier, Phys. Rev. B **52**, 1162 (1995); H. Courtois, Ph. Gandit, D. Mailly, and B. Pannetier, Phys. Rev. Lett. **76**, 130 (1996).
[25] A. F. Volkov, Phys. Rev. Lett. **74**, 4730 (1995).
[26] F. Zhou, B. Spivak, and A. Zyuzin, Phys. Rev. B **52**, 4467 (1995).